Hindawi Publishing Corporation
International Journal of Antennas and Propagation
Volume 2014, Article ID 761084, 7 pages
http://dx.doi.org/10.1155/2014/761084

Research Article

"Three Crossings" Compensations of the High Speed Moving MIMO Radar

Cheng Luo and Zishu He

School of Electronic Engineering, University of Electronic Science and Technology of China, Chengdu 611731, China

Correspondence should be addressed to Cheng Luo; genielc@aliyun.com

Received 15 November 2013; Revised 1 February 2014; Accepted 12 February 2014; Published 10 April 2014

Academic Editor: Wen-Qin Wang

The problems of the "Three Crossings" motions and compensations for the moving target of the high speed moving MIMO radar are studied. Firstly, the space model is established to describe the problems by educing the equations of delay and transmitting pattern, which are changing with time. The echo characteristics are analyzed and the formulas of the "Three Crossings" are given. Secondly, a compensation method, which uses the fractional Fourier transform (FrFT) to compensate the crossing Doppler-cell and the preprocess to compensate the crossing range-cell and crossing-beam, is proposed. This method could compensate the "Three Crossings" simultaneously with little complexity of calculation because the preprocess deals only with the transmitting signals. Lastly, the phantom antenna array is employed in the simulations, the working model of "sparse transmitting dense receiving" is applied to the simulation of crossing-beam, and the results of simulations demonstrate the validity and the practicability of the method of combining the preprocess and the FrFT to compensate "Three Crossings."

1. Introduction

The aircrafts are moving faster and faster as the development of the aviation technology, some of them could attain a velocity more than mach 10, and the maneuverability is becoming stronger too, which make the moving targets much more difficult to be searched, detected, and tracked by radar. Long time accumulation could increase the SNR output and the performance of detection, but adding accumulation time may cause "Three Crossings", which means crossing Doppler-cell, crossing range-cell, and crossing-beam. The "Three Crossings" ruin the coherence of the echo. In order to accumulate coherently to get the best detection ability, the "Three Crossings" must be compensated before the accumulation.

Some valuable studies have been proposed for the crossing Doppler-cell and crossing range-cell [1–8], but most of them could compensate only one of these crossings. The narrow beam of the phase array (PA) radar limited the study about the crossing-beam, for PA radar cannot compensate the crossing-beam; so far there is no reference for this study. The MIMO radar transmits orthogonal signals to form a low amplitude but wide beam to cover the whole surveillance area [9–11]. Even though the "Three Crossings" happen simultaneously, the MIMO radar can receive all the echoes without any energy loss. So, the MIMO radar produces the qualification for the study of the "Three Crossings," especially the crossing-beam.

In this paper, the "Three Crossings" of the target detected by a high-speed moving MIMO radar are studied. A space model is established firstly to educe the equations about how the delay and the transmitting pattern change with the time. Secondly, an analysis of the echo is proposed to show the "Three Crossings" of the target. Thirdly, the preprocessing method [12] is employed to compensate the crossing range-cell and the crossing-beam, while the fractional Fourier transform (FrFT) [13] is employed to compensate the crossing Doppler-cell. A performance brief analysis about the compensation mismatching is proposed after all this, and the simulation results are produced at last.

2. Space Model

At time t, the radar lies at point P with the height of H and moves along the Y-axis with a high speed v_r, while the target

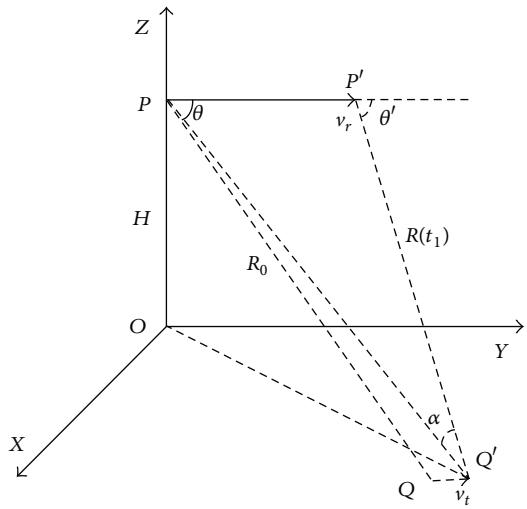

Figure 1: The space geometry relationship of the MIMO radar and the detected target.

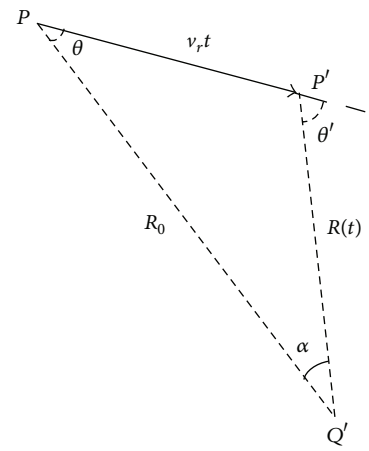

Figure 2: The changing angle.

lies at point Q and moves with a low speed v_t, assuming that v_r is much larger than v_t. Let the distance of the radar and the target $PQ = R_0$; the angle between the direction of the radar and PQ is θ. After t_1, the transmitting signal propagates to the point where the target lies; assume that the point is Q', the radar moves to point P', and the distance becomes $R(t_1)$. Because the target moves very slowly, the range QQ' is very small, PQ and PQ' are nearly the same, and angle $\angle P'PQ$ and angle $\angle P'PQ'$ are almost equal to each other, then we can assume that $PQ' = PQ = R_0$ and $\angle P'PQ' = \angle P'PQ = \theta$. The space geometry relationship of the MIMO radar and the detected target is shown in Figure 1.

According to the cosine theorem, $R(t_1)$ can be calculated; after Taylor expandedness, the delay of the echo should be

$$\tau(t) = \frac{2R_0}{c} + \frac{-2v}{c-v}\left(t - \frac{R_0}{c}\right) + \frac{ac^2}{(c-v)^3}\left(t - \frac{R_0}{c}\right)^2, \quad (1)$$

where v is the relative velocity, c is the velocity of light, and a is the acceleration. Educe a further step; (2) can be gotten as follows:

$$\begin{aligned} t - \tau(t) &= t - \frac{2R_0}{c} + \frac{2v}{c-v}\left(t - \frac{R_0}{c}\right) - \frac{ac^2}{(c-v)^3}\left(t - \frac{R_0}{c}\right)^2 \\ &= \frac{c+v}{c-v}t - \frac{c+v}{c-v}\frac{2R_0}{c+v} - \frac{ac^2}{(c-v)^3}t^2 \\ &= kt - kt_0 - pt^2, \end{aligned} \quad (2)$$

where

$$k = \frac{c+v}{c-v}, \qquad t_0 = \frac{2R_0}{c+v}, \qquad p = \frac{ac^2}{(c-v)^3}. \quad (3)$$

Extracting the triangle $PP'Q'$, in the whole surveillance period, the changing angle from the target to the radar is equal to α, as is shown in Figure 2.

Assuming that α is constant in one pulse repeat interval (PRI) and variable between each PRI, the MIMO radar has an M elements transmitting uniform linear array (ULA) and an N elements receiving ULA; L pulses are transmitted in the accumulation period. So, the phase matrixes of the steering vectors of the transmitting and receiving arrays are

$$\begin{aligned} \boldsymbol{\Psi}_T &= \left[\boldsymbol{\psi}(t_1), \boldsymbol{\psi}(t_2), \ldots, \boldsymbol{\psi}(t_L)\right]^T \\ &= \begin{bmatrix} \psi_1(t_1) & \psi_1(t_2) & \cdots & \psi_1(t_L) \\ \psi_2(t_1) & \psi_2(t_2) & \cdots & \psi_2(t_L) \\ \vdots & \vdots & \ddots & \vdots \\ \psi_M(t_1) & \psi_M(t_2) & \cdots & \psi_M(t_L) \end{bmatrix}^T, \end{aligned} \quad (4)$$

$$\begin{aligned} \boldsymbol{\Psi}_R &= \left[\boldsymbol{\Phi}(t_1), \boldsymbol{\Phi}(t_2), \ldots, \boldsymbol{\Phi}(t_L)\right]^T \\ &= \begin{bmatrix} \phi_1(t_1) & \phi_1(t_2) & \cdots & \phi_1(t_L) \\ \phi_2(t_1) & \phi_2(t_2) & \cdots & \phi_2(t_L) \\ \vdots & \vdots & \ddots & \vdots \\ \phi_N(t_1) & \phi_N(t_2) & \cdots & \phi_N(t_L) \end{bmatrix}^T, \end{aligned} \quad (5)$$

where the phase of the mth transmitting channel is

$$\psi_m(t_l) = \frac{2\pi(m-1)d_t}{\lambda}\sin\left[\alpha_1(t_l)\right], \quad m = 1 \sim M, \quad l = 1 \sim L \quad (6)$$

and the phase of the nth receiving channel is

$$\phi_n(t_l) = \frac{2\pi(n-1)d_r}{\lambda}\sin\left[\alpha_2(t_l)\right], \quad n = 1 \sim N, \quad l = 1 \sim L. \quad (7)$$

The angles α_1 and α_2 are the α in Figure 2. Assume that, after b PRI, the angle changes, so t_l should be

$$t_l = \left\lceil \frac{l}{b} \right\rceil T, \quad l = 1 \sim L, \tag{8}$$

where T could be any moment in the radar period T_r. According to the cosine theorem, the $\sin\alpha$ can be calculated in the triangle $PP'Q'$; put $\sin\alpha$ into (6); then we can get

$$\begin{aligned} \psi_m(t_l) = &\left(1 + \frac{v_r}{R_0}\left\lceil \frac{l}{b} \right\rceil T\cos\theta\right)\frac{v_r}{R_0}\left\lceil \frac{l}{b} \right\rceil T \\ &\cdot \frac{2\pi(m-1)\,d\sin\theta}{\lambda}, \\ &m = 1 \sim M, \\ &l = 1 \sim L. \end{aligned} \tag{9}$$

If the transmitting array and the receiving array are the same, $\sin[\alpha_2(t_l)]$ would have the same formula with $\sin[\alpha_1(t_l)]$, so (9) can be used for $\phi_n(t_l)$ too.

3. Echo Analysis

The transmitting signal can be expressed as

$$\mathbf{S} = [\mathbf{s}_1(t), \ldots, \mathbf{s}_L(t)] = \begin{bmatrix} s_{11}(t), \ldots, s_{1M}(t) \\ s_{21}(t), \ldots, s_{2M}(t) \\ \vdots \\ s_{L1}(t), \ldots, s_{LM}(t) \end{bmatrix}^T, \tag{10}$$

where the signal transmitted by the mth element at the lth period is

$$s_{lm}(t) = \mathrm{rect}\left(\frac{t - lT_r}{T_p}\right) s_{bm}(t - lT_r)\, e^{j2\pi f_c t}, \tag{11}$$

where $s_{bm}(t)$ denotes the transmitted baseband signal. The echo received by the nth channel after mixing should be

$$\begin{aligned} s_{r\_ln}(t) = &\sum_{m=1}^{M} \mathrm{rect}\left[\frac{t - \tau(t) - lT_r}{T_p}\right] s_{bm}[t - \tau(t) - lT_r] \\ &\times e^{-j2\pi f_c \tau(t)} e^{j\psi_m(t_l)} \cdot e^{j\phi_n(t_l)} + v_n(t). \end{aligned} \tag{12}$$

In this paper, the clutter is ignored to focus on the "Three Crossings" and their compensations; the clutter compression in this case of the airborne MIMO radar, including the clutter diffusing and agglomerating, will be discussed in another paper, so $v_n(t)$ in (12) only stands for the noise.

Name the rectangle function in (12) as $f(t)$, so

$$f(t) = \mathrm{rect}\left[\frac{t - \tau(t) - lT_r}{T_p}\right] = \mathrm{rect}\left(\frac{kt - kt_0 - pt^2 - lT_r}{T_p}\right). \tag{13}$$

Let the numerator in (13) be 0; the front edge in the fast-slow time domain of the echo can be calculated as

$$\widehat{t}(l) = \frac{pT_r^2}{k^3} l^2 + \left(\frac{1}{k} - 1 - \frac{2pT_r t_0}{k^2}\right) lT_r + (2k-1)\, t_0 + \frac{pt_0^2}{k}. \tag{14}$$

The echo envelope will move in the fast-slow time domain as the number of the pulse increases, according to (14), so the range migration would happen in this case.

Name the baseband signal and the first exponential function in (12) as $g(t)$, so

$$g(t) = \sum_{m=1}^{M} s_{bm}[t - \tau(t) - lT_r]\, e^{-j2\pi f_c \tau(t)}. \tag{15}$$

Here, the delay $\tau(t)$ is a quadric polynomial and the Doppler-frequency of the echo $f_d(t)$ would be a function of time, which would make the coherence of the echo be destroyed; that is to say, the Doppler migration would happen in this case.

Name the last two exponential functions in (12) as $h(t)$, so

$$h(t) = \sum_{m=1}^{M} e^{j\psi_m(t_l)} \cdot e^{j\phi_n(t_l)}. \tag{16}$$

According to (4)~(9), we have

$$\psi_m(t_{l_1}) \neq \psi_m(t_{l_{1+b}}), \qquad \phi_n(t_{l_1}) \neq \phi_n(t_{l_{1+b}}). \tag{17}$$

That is to say, after b PRI, the target moves into the next beam and the crossing-beam would happen in this case.

4. Compensation Methods

In this paper, the preprocess method and the FrFT are employed to compensate the "Three Crossings." The preprocess method compensates the range migration by combining the direct digital synthesis (DDS) technology to control the transmit signal elaborately, that is, to regulate the pulse width of the transmitting signal to make the echo envelopes be aligned automatically in the fast-slow time domain. The beam-crossing is compensated by preprocessing the transmitting signal too. Based on the algorithm of the preprocess, the conjugate of the transmitting pattern is added in the transmitting signals to make the transmitting angles be compensated at the target.

From $p = ac^2/(c-v)^3 \approx a/c$, p provides little effect on the range migration, so $f(t)$ can be approximated as

$$f(t) = \mathrm{rect}\left(\frac{kt - kt_0 - lT_r}{T_P}\right). \tag{18}$$

So, the new transmitting signal can be written as

$$\begin{aligned} s_{lm}(t) = &\mathrm{rect}\left(\frac{t/k - lT_r}{T_p}\right) s_{bm}\left(\frac{t}{k} - lT_r\right) e^{-j\psi_m(t_l)} e^{j2\pi f_c t}, \\ &m = 1 \sim M. \end{aligned} \tag{19}$$

Then, the added signal at the target should be

$$s_{T\_lm}(t) = \sum_{m=1}^{M} \text{rect}\left[\frac{(t-t_1)/k - lT_r}{T_p}\right] s_{bm} \times \left[\frac{(t-t_1)}{k} - lT_r\right] e^{j2\pi f_c(t-t_1)}, \tag{20}$$

where t_1 is the transmitting delay from radar to the target. So, the echo after mixing should be

$$s_{r\_ln}(t) = \sum_{m=1}^{M} \text{rect}\left(\frac{\hat{t}-t_0}{T_P}\right) s_{bm}\left[\frac{t-\tau(t)}{k} - lT_r\right] \times e^{-j2\pi f_c \tau(t)} e^{j\phi_n(t_l)} + v_n(t). \tag{21}$$

The front edge of the echo envelopes in the fast-slow time domain is a constant t_0, which means the echo envelopes are aligned, so the range-cell crossing is compensated.

After the receiving beam forming, we have

$$\begin{aligned} s_{r\_l}(t) &= \sum_{n=1}^{N} s_{r\_ln}(t)\, e^{-j\phi_n(t_l)} \\ &= \sum_{n=1}^{N}\sum_{m=1}^{M} \text{rect}\left(\frac{\hat{t}-t_0}{T_P}\right) s_{bm}\left[\frac{t-\tau(t)}{k} - lT_r\right] e^{-j2\pi f_c \tau(t)} \\ &\quad + \sum_{n=1}^{N} v_n(t). \end{aligned} \tag{22}$$

In (22), the transmitting pattern is canceled by the receiving pattern, so the beam-crossing is compensated. Next, the FrFT is employed to compensate the Doppler-cell crossing, which would make the phases of the echo contain only constant and one-order polynomial; the result should be

$$s_{r\_l}(t) = \sum_{n=1}^{N}\sum_{m=1}^{M} \text{rect}\left(\frac{\hat{t}-t_0}{T_P}\right) s_{bm}(\lambda_1 t + \lambda_0) \times e^{-j2\pi f_c(\xi_1 t + \xi_0)} + \sum_{n=1}^{N} v_n(t), \tag{23}$$

where λ_1 and ξ_1 are the coefficients of the one-order polynomial of t and λ_0 and ξ_0 are constants.

In (23), the echo envelopes are aligned in the fast-slow time domain, the orders of the echo phases are less than 2, and the pattern is constant, so after the processes of the preprocess and the FrFT, the "Three Crossings" are corrected, echo pulses are coherent, and the highest accumulation output can be gotten after the matched filter and FFT.

5. Simulations

The LFM signal is employed in the simulations. The conditions are as follows: the PRI is 1 ms, the pulse width is 0.1 ms, the original range between the radar and the target is 100 km, the velocity of the radar platform is 1 km/s, $\theta = \pi/6$, the number of the transmitting antennas is 2, the bandwidth is 0.2 MHz, the frequency interval of the channels is 0.2 MHz, the number of the pulses is 500, the sample frequency is 1 MHz, the carrier frequency is 2 GHz, and the zero intermediate frequency is 0.2 MHz. After a little simple calculation, the original relative velocity is $v_r \approx 866$ m/s, the acceleration is 5 m/s^2, during the accumulation period, and the range between the radar and the target shifts $\Delta R \approx 433.6$ m.

The relative range shifts about 450 m in Figure 3(a); it is quite close to the number calculated by equation. The MTD result expands in the velocity dimension because of the Doppler shift.

After the range compensation, the peaks of the MF results are superposition, but the MTD result is still expanding. From Figure 4, the range-cell crossing has been compensated, but the Doppler-cell crossing still exists.

After the range and Doppler compensations are done, the MF results are totally superposition and the MTD result is an ideal thumb pin; then we can gain the highest accumulation output (see Figure 5).

When the beam-crossing happens, three conditions are satisfied generally; those are as follows: (1) the number of the transmitting elements is large, (2) the relative range between the radar and the target is not too far away, and (3) the vertical velocity is high. So, the relative range is reset as 20 km, the velocity of the radar is reset as 3000 m/s, the number of the transmitting elements is 10, and the PRI changes into 2 ms. The phantom element [14] is employed in the transmitting array and the interval distance is equal to the product of the number of the transmitting elements and the half of the wavelength, which could expand the transmitting caliber to 100 transmitting elements to decrease the width of the transmitting main lobe. It can be calculated that the width of the main lobe is about 0.731°, the shift of the angle in one PRI is 0.0744°, after 100 PRI, and the target moves across 2.0362 beams.

The accumulations before and after compensating the beam-crossing, on condition that the range-cell crossing and the Doppler-cell crossing have been compensated, are shown in Figure 6, and the accumulations are normalized by the accumulation result before compensating the beam-crossing. It is obvious to see that the peak after compensation is twice higher than that before, which is consistent with the case that the target moves across about 2 beams.

To prove the validity of the precompensation method, simulations are taken under the main conditions that the numbers of the transmitting and receiving channels are $M = N = 4$, the number of the transmitting pulses is $L = 200$, the radar PRI is $T_r = 1$ ms, the pulse width is $T_p = 50\,\mu$s, the original distance of the radar and the target is $R_0 = 100$ km, and the real relative velocity is $v_0 = 4$ km/s. Consider that it is difficult to know the real relative velocity in practice, so in order to check the performance of the precompensation when $v \neq v_0$, four different possible relative velocities are selected as the compensation velocities and $v = 4, 5, 6, 7$ km/s; for the

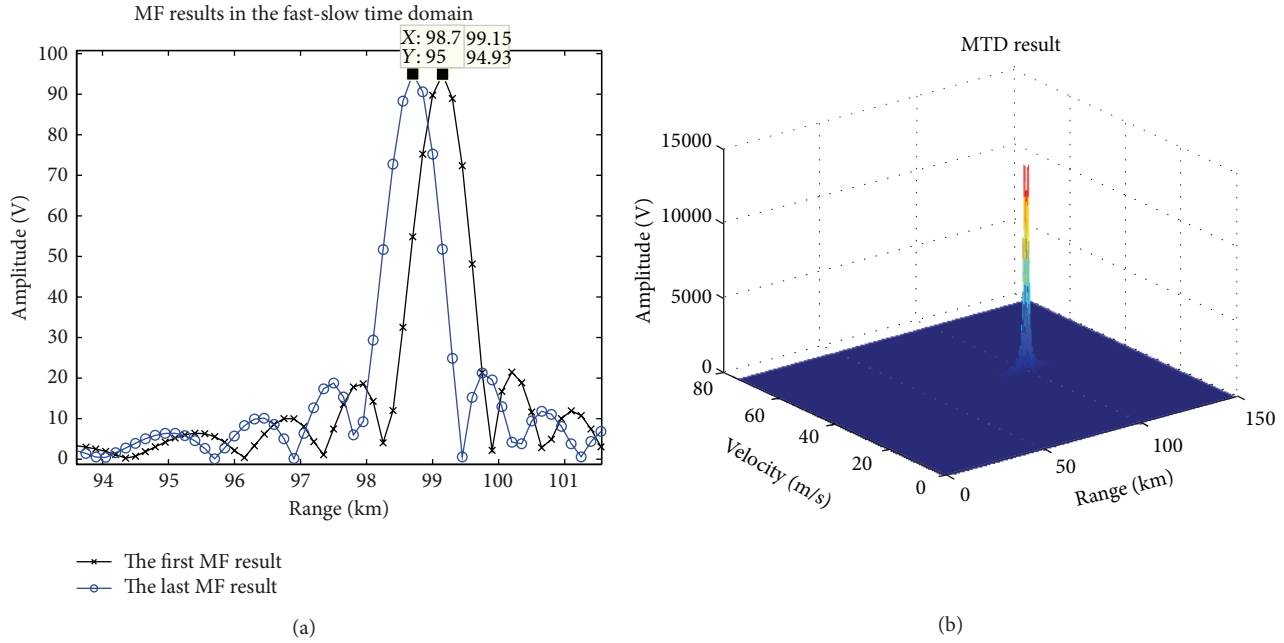

Figure 3: The matched filter (MF) and MTD results without any compensation.

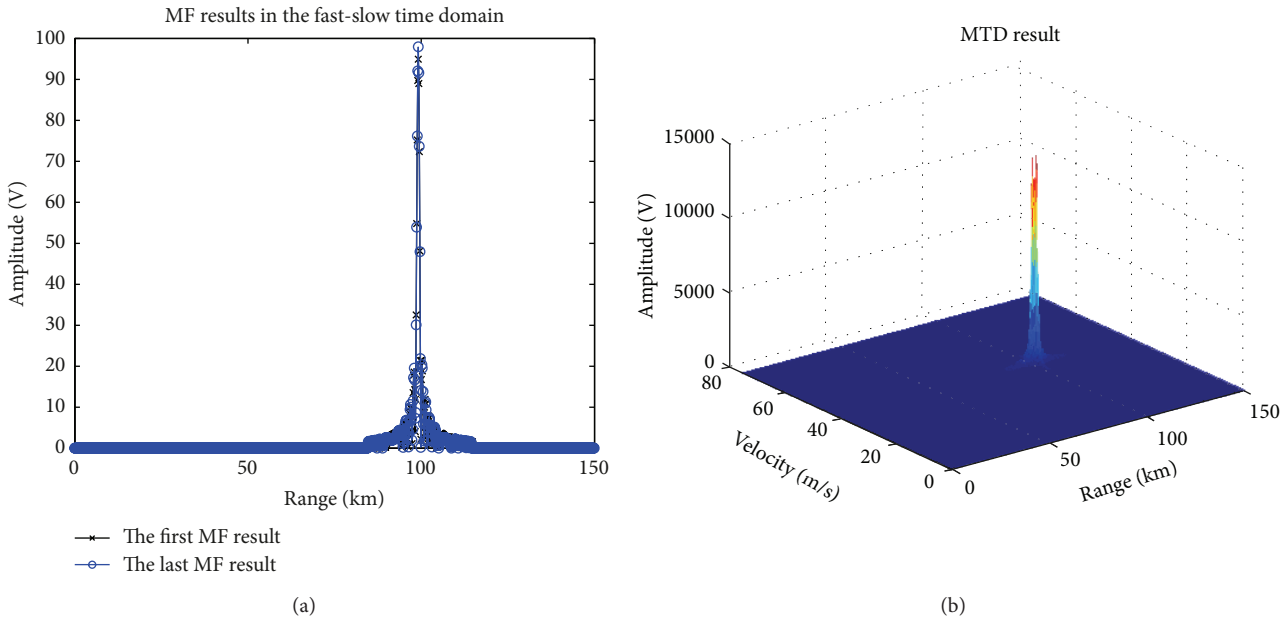

Figure 4: The matched filter and MTD results after range compensation.

symmetry, the performances of these velocities should be the same, respectively, to $v = 4, 3, 2, 1$ km/s.

Firstly, the accumulation results of different compensation velocities are shown in Figure 7. It is easy to see that when the compensation velocity is more different from the real relative velocity, the accumulation result is wider and the peak is lower, which means the compensation performance is worse. When the compensation velocity is 7 km/s, the peak of the accumulation is nearly 3 dB less than the accumulation of $v = 4$ km/s. So, when the difference between the real relative velocity and the compensation velocity is less than 3 km/s, the accumulation performance is acceptable. At the same time, one could see that there is a good velocity difference tolerance.

Secondly, the detection probabilities of the four different compensation velocities are shown in Figure 8. Corresponding to the results in Figure 7, at the same SNR value, when the compensation velocity is more different from the real relative velocity, the detection probability is lower. If there is

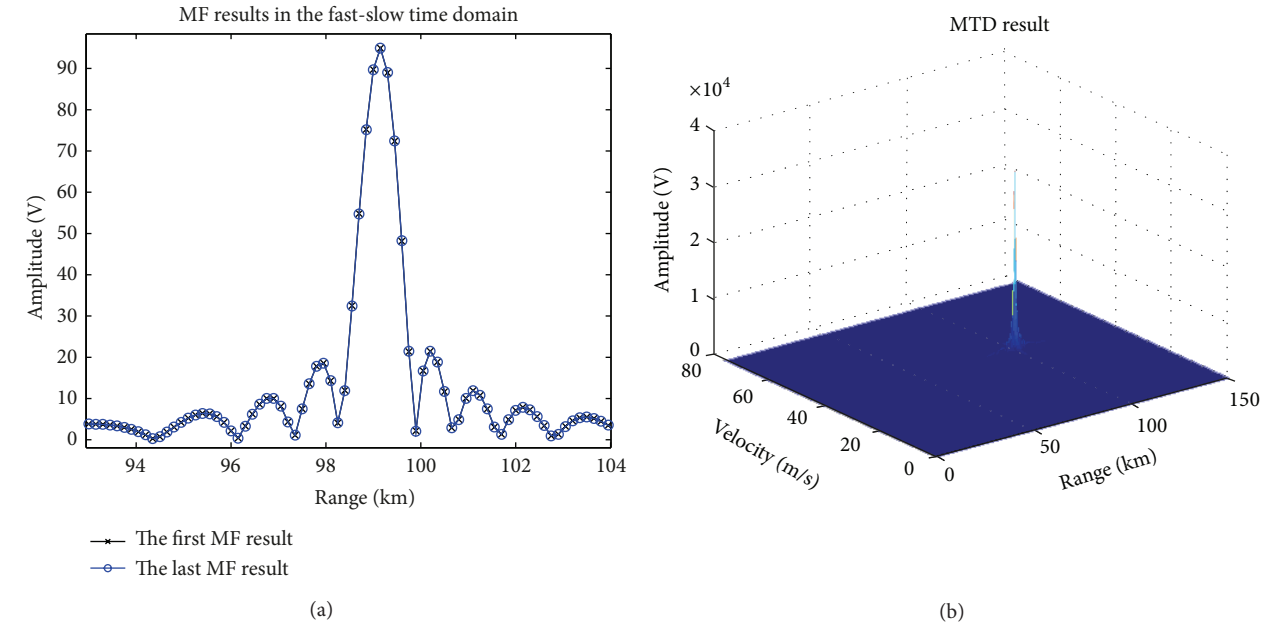

Figure 5: The matched filter and MTD results after range and Doppler compensations.

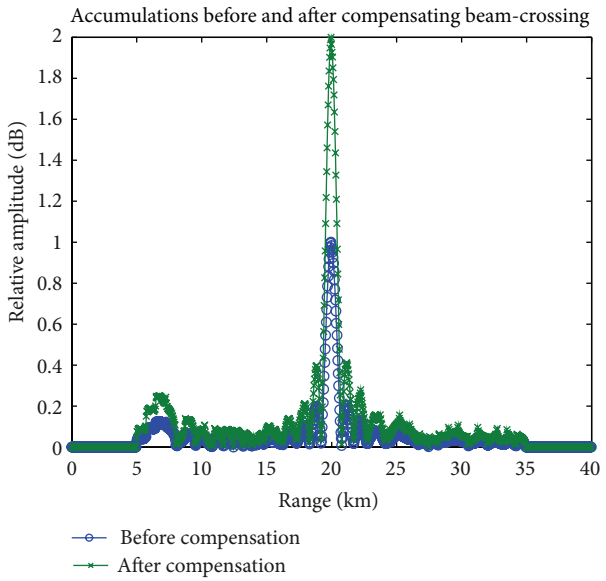

Figure 6: Accumulation results before and after the beam-crossing compensations.

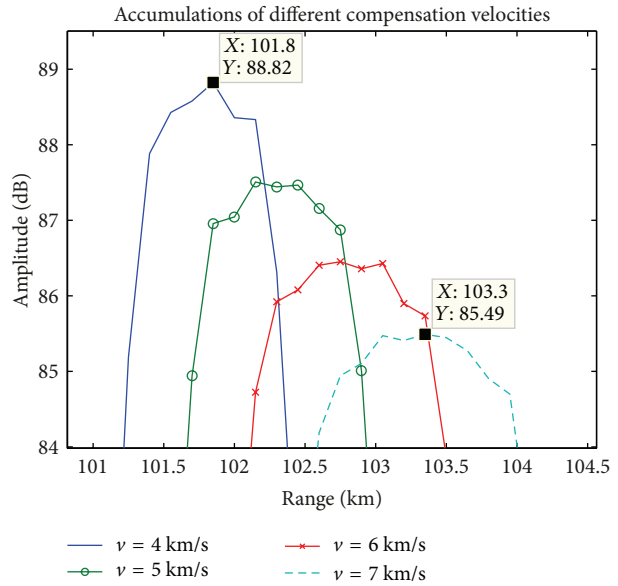

Figure 7: Accumulations of four different compensation velocities.

no compensation, the scenario is the same to the $v = 8$ km/s or $v = 0$ km/s and the detection performance would be even worse than the one when $v = 7$ km/s.

From these two groups of simulation results, one can figure out that the precompensation can compensate the range migration valid in a tolerance of the difference between the real relative velocity and the compensation velocity. The detection probability at 90% after compensation when $v = v_0$ is about 7 dB or 8 dB better than the one when these two velocities are 3 km/s different.

6. Conclusion

As the developments of the velocity and the maneuverability of aircrafts, the "Three Crossings" are becoming bigger problems for the MTD. Traditional radars cannot compensate the beam-crossing, so no article discussed this problem. MIMO radar, which transmits a wide beam, provides the probability to achieve the compensation of the beam-crossing. In this paper, the "Three Crossings" are discussed simultaneously based on the airborne MIMO radar system. To detect the moving target, the characteristic of the echo is analyzed, the

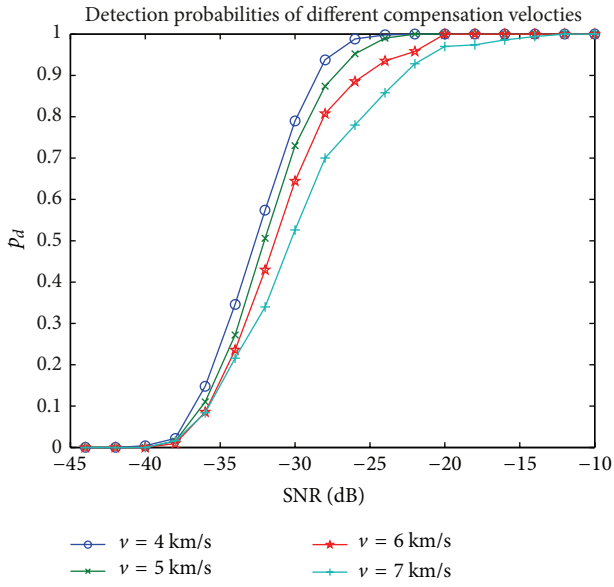

FIGURE 8: Detection probabilities of four different compensation velocities.

"Three Crossings" model is proposed, and then the preprocessing method and the FrFT are employed to compensate the "Three Crossings." The simulation results show that these two methods can compensate the "Three Crossings" validly; the accumulation peak is significantly higher after the compensations. Even when the compensation velocity is not exactly the same with the real one, the compensation performance is also acceptable within a large velocity tolerance.

Conflict of Interests

The authors declare that there is no conflict of interests regarding the publication of this paper.

Acknowledgments

The authors would like to thank all the editors and referees for their suggestions and advices. This work is supported by the National Natural Science Foundation of China (no. 11076006, no. 61032010, and no. 61101173).

References

[1] R. P. Perry, R. C. Dipietro, and R. L. Fante, "SAR imaging of moving targets," *IEEE Trans on AES*, vol. 32, no. 1, pp. 188–200, 1999.

[2] Y. Liu, H. Meng, G. Li, and X. Wang, "Velocity estimation and range shift compensation for high range resolution profiling in stepped-frequency radar," *IEEE Geoscience and Remote Sensing Letters*, vol. 7, no. 4, pp. 791–795, 2010.

[3] Y. Boers and J. N. Driessen, "Multi-target particle filter track before detect application," *IET Proceeding of Radar Sonar Navigation*, vol. 151, no. 6, pp. 351–357, 2004.

[4] J. Su, M. Xing, G. Wang, and Z. Bao, "High-speed multi-target detection with narrowband radar," *IET Radar, Sonar and Navigation*, vol. 4, no. 4, pp. 595–603, 2010.

[5] Y. Liu, H. Meng, G. Li, and X. Wang, "Velocity estimation and range shift compensation for high range resolution profiling in stepped-frequency radar," *IEEE Geoscience and Remote Sensing Letters*, vol. 7, no. 4, pp. 791–795, 2010.

[6] Y. Boers and J. N. Driessen, "Multi-target particle filter track before detect application," *IEE Proceedings of Radar Sonar Navig*, vol. 151, no. 6, pp. 351–357, 2004.

[7] F. G. Geroleo and M. Brandt-Pearce, "Detection and estimation of LFMCW radar signals," *IEEE Transactions on Aerospace and Electronic Systems*, vol. 48, no. 1, pp. 405–418, 2012.

[8] J. Guan, X. -L. Chen, Y. Huang, and Y. He, "Adaptive fractional Fourier transform-based detection algorithm for moving target in heavy sea clutter," *IET Radar, Sonar and Navigation*, vol. 6, no. 5, pp. 389–401, 2012.

[9] D. J. Rabideau and P. Parker, "Ubiquitous MIMO multifunction digital array radar," in *Conference Record of the 37th Asilomar Conference on Signals, Systems and Computers*, vol. 1, pp. 1057–1064, November 2003.

[10] P. W. Moo, "Multiple-input multiple-output radar search strategies for high-velocity targets," *IET Radar, Sonar and Navigation*, vol. 5, no. 3, pp. 256–265, 2011.

[11] A. Hassanien, S. A. Vorobyov, and A. B. Gershman, "Moving target parameters estimation in noncoherent MIMO radar systems," *IEEE Transactions on Signal Processing*, vol. 60, no. 5, pp. 2354–2361, 2012.

[12] C. Luo, J. Li, H. M. Liu, and Z. S. He, "Compensation method for envelop migration of MIMO radar high speed moving target based on transmit signal pre-process," in *International Workshop on Microwave and Millimeter Wave Circuits and System Technology (MMWCST '12)*, pp. 1–4, Cheng Du, China, 2012.

[13] H.-B. Sun, G.-S. Liu, H. Gu, and W.-M. Su, "Application of the fractional Fourier transform to moving target detection in airborne SAR," *IEEE Transactions on Aerospace and Electronic Systems*, vol. 38, no. 4, pp. 1416–1424, 2002.

[14] B. J. Donnet and I. D. Longstaff, "MIMO radar, techniques and opportunities," in *Proceedings of the 3rd European Radar Conference*, pp. 112–115, Manchester, UK, September 2006.